Neuron
Article

Functional Differentiation of Memory Retrieval Network in Macaque Posterior Parietal Cortex

Kentaro Miyamoto,[1] Takahiro Osada,[1,4] Yusuke Adachi,[1,4] Teppei Matsui,[1,2] Hiroko M. Kimura,[1] and Yasushi Miyashita[1,2,3,*]
[1]Department of Physiology, The University of Tokyo School of Medicine, 7-3-1 Hongo, Bunkyo-ku, Tokyo 113-0033, Japan
[2]Department of Physics, The University of Tokyo School of Science, 7-3-1 Hongo, Bunkyo-ku, Tokyo 113-0033, Japan
[3]CREST, JST, Kawaguchi, Saitama 332-0012, Japan
[4]These authors contributed equally to this work
*Correspondence: yasushi_miyashita@m.u-tokyo.ac.jp
http://dx.doi.org/10.1016/j.neuron.2012.12.019

SUMMARY

Human fMRI studies revealed involvement of the posterior parietal cortex (PPC) during memory retrieval. However, corresponding memory-related regions in macaque PPC have not been established. In this monkey fMRI study, comparisons of cortical activity during correct recognition of previously seen items and rejection of unseen items revealed two major PPC activation sites that were differentially characterized by a serial probe recognition paradigm: area PG/PGOp in inferior parietal lobule, along with the hippocampus, was more active for initial item retrieval, while area PEa/DIP in intraparietal sulcus was for the last item. Effective connectivity analyses revealed that connectivity from hippocampus to PG/PGOp, but not to PEa/DIP, increased during initial item retrieval. The two parietal areas with differential serial probe recognition profiles were embedded in two different subnetworks of the brain-wide retrieval-related regions. These functional dissociations in the macaque PPC imply the functional correspondence of retrieval-related PPC networks in macaques and humans.

INTRODUCTION

Human imaging studies report the involvement of posterior parietal cortex (PPC), in addition to medial temporal lobe (MTL) and prefrontal cortex (PFC), in memory retrieval (Curtis and D'Esposito, 2003; Miyashita, 2004; Squire et al., 2004). Multiple areas in PPC show retrieval-related activation when human individuals correctly recognize previously seen items as compared with correctly identifying unseen new items ("old/new effect") (Konishi et al., 2000; Vilberg and Rugg, 2008). fMRI studies have dissociated these PPC areas by differences in their cognitive function (Eichenbaum et al., 2007; Wagner et al., 2005), as well as by differences in their functional/anatomical connectivity with MTL and PFC (Nelson et al., 2010; Rushworth et al., 2006). However, unlike MTL and PFC, in which neuropsychological evidence for memory function is abundant (for reviews see Baldo and Shimamura, 2002; Squire et al., 2004), neuropsychological studies have only recently shown that damage to PPC causes mild impairment in episodic retrieval (Davidson et al., 2008). Neuropsychological clues that dissociate the retrieval processes in PPC remain insufficient due to the limited number of available cases with damage in specific PPC subregions.

To bridge the gap between the results in human fMRI and neuropsychology, it would be beneficial to investigate memory retrieval-related PPC function in nonhuman primates, where finer-scale, well-controlled experimental techniques are available (Osada et al., 2008). Macaque PPC has been investigated as a region responsible for multiple functions including visuospatial processing (Vanduffel et al., 2002), the saccadic system (Kagan et al., 2010; Koyama et al., 2004), attention, intention, and decision-making (Bisley and Goldberg, 2010). However, the functional localization of retrieval-related neural activity in PPC remains unknown in monkeys. Due to differences in cytoarchitectonic organization between human and macaque PPC (Husain and Nachev, 2007), it is difficult to infer retrieval-related PPC areas in monkeys based purely on anatomical information. Awake monkey fMRI, which captures whole-brain activity related to specific cognitive processes using an identical paradigm to human studies, is the most suitable technique to localize memory retrieval-related regions in the macaque cerebral cortex (Kagan et al., 2010; Koyama et al., 2004; Logothetis et al., 1999; Maier et al., 2008; Nakahara et al., 2002; Pinsk et al., 2005; Tsao et al., 2003).

In the present fMRI study, we first identified the retrieval-related cortical regions of monkeys that demonstrated the old/new effect. We then characterized and compared the response profiles of the identified retrieval-related regions of monkeys based on the serial position effect. In the task, monkeys were required to view a list of serially presented items and to judge whether the test item was seen in any item position of the list (old/new judgment). Behaviorally, in both monkeys and humans, memory accuracy is known to show primacy and recency effects that are accompanied by typical U-shaped serial position curves; that is, the accuracy of the retrieval of the first items (primacy effect) and the accuracy of the retrieval of the last items (recency effect) are higher than that of retrieval of other items (Wright et al., 1985; see also Figure 1). Damage in bilateral hippocampi specifically impaired primacy effect but not recency

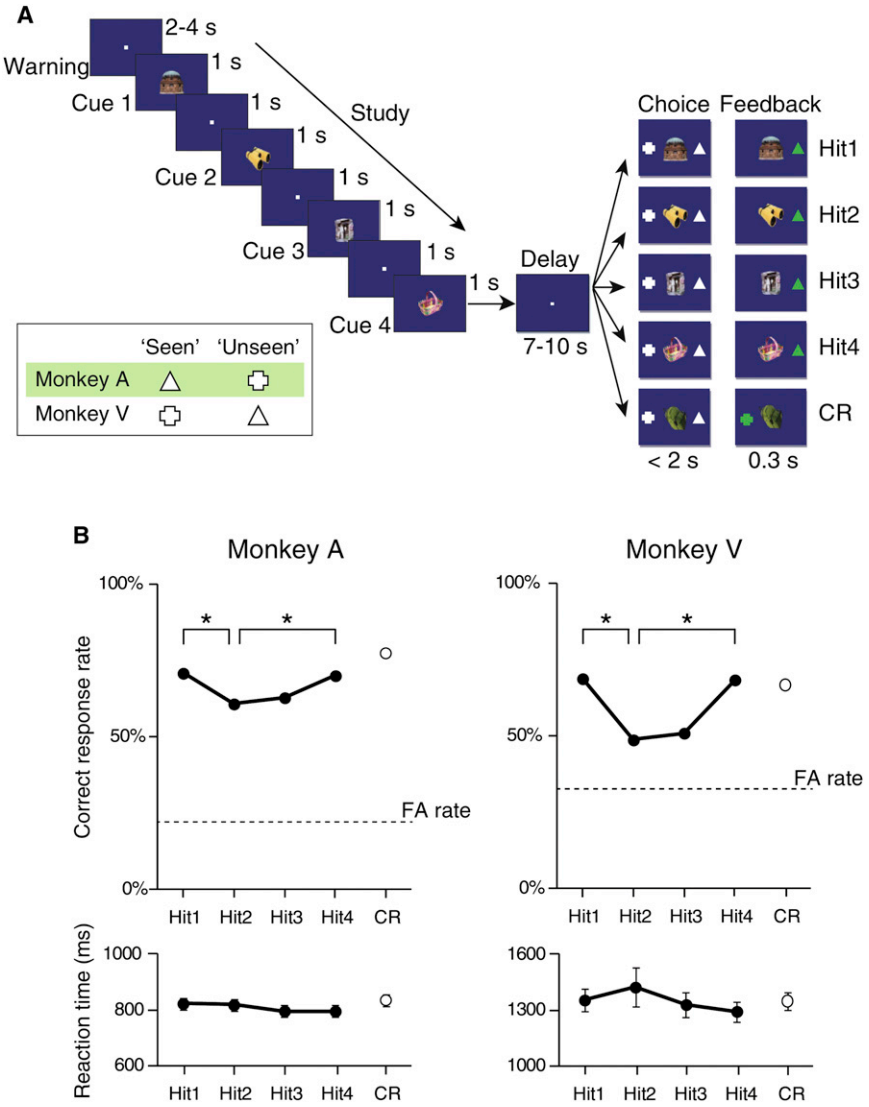

Figure 1. Serial Probe Recognition Task and Behavioral Performance of Monkeys

(A) Trial structure in the serial probe recognition task. In each trial, monkeys pulled the joystick to initiate the trial (Warning), and then four objects to study were sequentially presented (Cue1–4). After a 7–10 s delay (Delay), two choice symbols were presented with a test object (Choice). The symbols, a triangle and a cross, were defined as "seen" and "unseen" symbols for each monkey (see "inset table"). Monkeys were required to select the "seen" (or "unseen") symbol if the test object was (was not) included in the studied list of objects. The classification of Hit and CR trials in the case of the symbol definition in monkey A is shown here.

(B) Serial position curves of behavioral performance for each monkey during scanning sessions. Upper panels show serial position curves for the percentage of correct responses. Each dot represents the Hit rate (●) or CR rate (○). In both monkeys, the Hit rate showed a U-shaped curve as a function of the item position (i.e., the position in the object list) in which the tested item (i.e., test object) was presented in the studied list. Hit rates for each item position significantly exceeded the FA rate (dashed line) (all $p < 0.05$). Lower panels show reaction times (●, Hit trials; ○, CR trials). *: $p < 0.05$ (chi-square test, Ryan's correction). Error bars: SEM. See also Figure S1.

effect in humans (Baddeley and Warrington, 1970). Human fMRI studies show that activity in hippocampus reflects the primacy effect (Huijbers et al., 2010; Talmi et al., 2005). These characteristics of the serial position effects also allowed us to characterize the retrieval-related areas in PPC in monkeys. In this study, the two retrieval-related parietal areas, one located in the inferior parietal lobule (IPL) and the other in the intraparietal sulcus (IPS), demonstrated mutually contrasting profiles depending on the item positions both in activation and task-evoked connectivity. This functional differentiation in the macaque PPC suggested the functional correspondence of the retrieval-related PPC networks in monkeys and humans.

RESULTS

Behavioral Results

We conducted fMRI in two macaque monkeys performing a single-probe recognition task (see Figure S1A available online) and a serial probe recognition task with a list of four items (Figure 1A). In these tasks, monkeys were required to judge whether or not the item in the choice period was seen on the list of items presented during the cue period. In the single-probe recognition task, "corrected recognition rate" (defined as "Hit rate" − "False Alarm [FA] rate") (Wagner et al., 1998) was significantly positive (chi-square test; $p < 0.001$ for both monkeys) (Figure S1B, upper panels), suggesting that the monkeys adequately distinguished seen items from unseen items based on items retrieved from memory. Hit rate and Correct Rejection (CR) rate were not significantly different (chi-square test; monkey A, $p = 0.63$; monkey V, $p = 0.31$). Reaction times for Hit and CR responses were not significantly different (paired t test (across sessions); monkey A, $t(23) = -1.44$, $p = 0.16$; monkey V, $t(25) = 1.26$, $p = 0.21$) (Figure S1B, lower panels). In the serial probe recognition task, the corrected recognition rate for each position of the cue item (Hit1 to Hit4) was significantly positive for both monkeys (chi-square test; $p < 0.05$, for each item of both monkeys) (Figure 1B, upper panels). In addition, the Hit rate was significantly different across the four item positions of the cue (chi-square test; monkey A, $\chi^2(3) = 9.05$, $p = 0.02$; monkey V, $\chi^2(3) = 9.98$, $p = 0.01$). Consistent with previous behavioral studies in humans and monkeys, U-shaped serial position curves of the percentage of correct responses were obtained in both monkeys, indicating

the presence of "primacy" and "recency" effects in the recognition task (Basile and Hampton, 2010; Wright et al., 1985). To test the statistical significance of primacy and recency effects in the U-shaped serial position curve, the accuracy on the first list position (Hit1), the last list position (Hit4) and the least accurate of the two middle positions (Hit2 or Hit3) were compared for each monkey (Basile and Hampton, 2010). For both monkeys, the Hit1 and Hit4 rates were significantly higher than the Hit2 rate, which was the least accurate (chi-square test; $p < 0.05$, Ryan's correction). Additionally, no significant difference between the Hit1 and Hit4 rates was observed in either monkey (chi-square test; $p > 0.5$, Ryan's correction). No significant main effect of the position on reaction time was observed (one-way repeated ANOVA [across sessions]; monkey A, $F(3,45) = 2.27$, $p = 0.09$; monkey V, $F(3,30) = 0.58$, $p = 0.63$) (Figure 1B, lower panels).

Identification of Retrieval-Related Regions

The cortical regions activated by correct recognition of previously presented items (Hit) compared to correct identification of previously unseen items (CR) in the single-probe recognition task in monkeys are shown in Figure 2A (Hit versus CR). In total, 47 significant activation peaks were detected (Table 1; $p < 0.01$, fixed effect, corrected for false discovery rate [FDR]). In the PPC, the strongest activation was found bilaterally in the IPS (PEa/DIP, see also "Nomenclatures of Retrieval-Related Areas in PPC" in Supplemental Text). In both monkeys, these bilateral peaks in the posterior IPS were located on the medial bank, which is more clearly confirmed in the activation maps generated from unsmoothed functional images (Figure S2; see Supplemental Experimental Procedures). The posterior IPL (PG/PGOp) was also activated bilaterally. In the frontal cortex, the anterior bank (area 45B) and posterior bank (area 6VR [ventral premotor, F5]) of bilateral inferior arcuate sulci were activated. The regions around the right principal sulcus (area 9/46V) and right superior arcuate sulcus (area 8B) were also significantly activated. Area 9/46V ($x = -16$, $y = 13$, $z = 8$, $t = 4.19$, $p < 0.001$, FDR corrected) and area 8B ($x = -15$, $y = 8$, $z = 15$, $t = 3.10$, $p < 0.01$, FDR corrected) were also significantly activated on the contralateral side, although the activation peak was located outside of these regions. In MTL regions, bilateral posterior hippocampi (pHC) and left middle hippocampus (mHC) were strongly activated. The right mHC was also activated ($x = -16$, $y = -15$, $z = -9$, $t = 3.34$, $p < 0.01$, FDR corrected), although the activation peak was located outside of this region. Figure 2B shows the regions that were significantly activated in both of the monkeys for Hit versus CR (conjunction null, $p < 0.05$, FDR corrected) (Friston et al., 2005; Nichols et al., 2005). This conjunction analysis showed that the majority of activated spots, especially in the parietal cortex, frontal cortex, and hippocampus, were duplicated in individual monkeys.

Neural Correlates of the Primacy and Recency Effects in Retrieval-Related Regions

Next, we examined if retrieval activities in the identified regions changed depending on the position of the cue item during the serial probe recognition task. To characterize retrieval-related activities in PPC, we first focused on the IPL (PG/PGOp) and the IPS (PEa/DIP), as well as the hippocampi (pHC, mHC) that were suggested to be related to the primacy effect in previous human studies (Baddeley and Warrington, 1970; for further details to focus on these areas, see Supplemental Text). We examined the effect of cue item position on the retrieval-related activities in each region by conducting an across-session repeated-measures multivariate ANOVA (MANOVA; four levels of retrieved cue item positions × two hemispheres × two monkeys). For the regions where MANOVA showed a significant main effect of retrieved cue item positions without significant interaction with either hemisphere or monkey, we then conducted regression analyses using a "primacy predictor" (n_p) and a "recency predictor" (n_r) (see Supplemental Experimental Procedures). In the bilateral hippocampi, MANOVA showed a significant main effect of retrieved cue item position ($F(3,22) = 3,60$, $p = 0.03$) for the retrieval activity, and the regression analyses revealed significant positive modulation to the first items ($\beta_p = 0.58 \pm 0.13$ [mean ± SEM], $t(51) = 4.24$, $p < 0.001$) with significant negative modulation to the last items ($\beta_r = -0.53 \pm 0.15$, $t(51) = -3.45$, $p = 0.002$) (Figures 3A, 3D, and 3E). Also in the bilateral PG/PGOp, MANOVA showed a main effect of retrieved cue item position ($F(3,22) = 3.25$, $p = 0.04$), and significant positive modulation was observed in response to the initial items ($\beta_p = 0.59 \pm 0.16$, $t(51) = 3.64$, $p = 0.001$) but not to the last items ($\beta_r = -0.35 \pm 0.15$, $F(1,24) = -2.22$, $p = 0.06$) (Figures 3B, 3D, and 3E). In the bilateral PEa/DIP, MANOVA showed a main effect of retrieved cue item position ($F(3,22) = 3.26$, $p = 0.04$). By contrast with hippocampi and PG/PGOp, significant positive modulation was observed in response to the last items ($\beta_r = 0.33 \pm 0.13$, $t(51) = 2.46$, $p = 0.03$) but not to the initial items ($\beta_p = 0.22 \pm 0.15$, $t(51) = 1.43$, $p = 0.31$) (Figures 3C, 3D, and 3E). These results indicate that retrieval-related activity in hippocampi and PG/PGOp reflected the primacy effect, whereas that of PEa/DIP reflected the recency effect.

Differential Increase in Effective Connectivity during Retrieval

To investigate whether the retrieved cue item position affects not only their activity but also the connectivity among these three retrieval-related regions, we conducted a psychophysiological interaction (PPI) analysis. When we located the PPI seed on the right pHC, comparisons of the retrieval of the initial items against that of the last items led to significantly increased effective connectivity with the right PG/PGOp ($p = 0.01$, family-wise error [FWE] corrected within PG/PGOp) but not with the right PEa/DIP ($p > 0.05$, FWE corrected) (Figure 3F, left panel). These results suggested that the right PG/PGOp connected more strongly with right pHC when the right pHC was highly activated for retrieval of the initial item than for retrieval of the last item. The same results were replicated in the left hemisphere (Figure 3F, middle panel): when the PPI seed was located on the left mHC, the retrieval of the initial item against the last led to significantly increased functional connectivity with the left PG/PGOp ($p = 0.04$, FWE corrected) but not with the left PEa/DIP ($p > 0.05$, FWE corrected). Thus, stronger functional connection from the hippocampus to the posterior IPL (PG/PGOp) during the retrieval of the initial cue item was replicated in both hemispheres (Figure 3F, right panel).

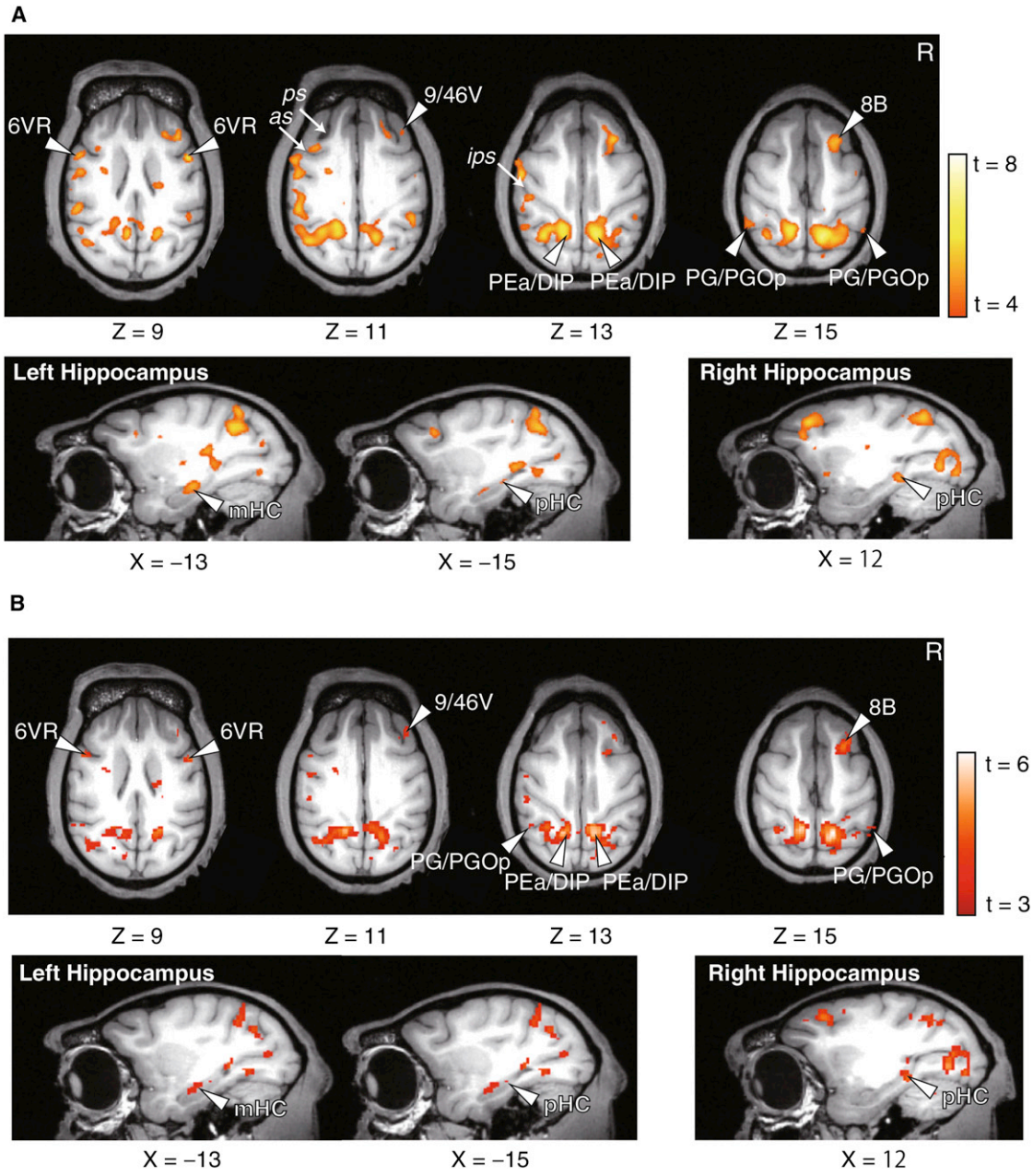

Figure 2. Memory Retrieval Regions in Macaque Cortex

(A) Activation maps (Hit > CR contrast) superimposed on transverse sections (upper panels) and sagittal sections (lower panels) ($t > 4.0$, $p < 0.001$, fixed effect, corrected by FDR). 6VR, ventral premotor; 9/46V, area 9/46V; PEa/DIP, area in intraparietal sulcus; 8B, area 8B; PG/PGOp, area in posterior inferior parietal lobule; mHC, middle hippocampus; pHC, posterior hippocampus; as, arcuate sulcus; ps, principal sulcus; ips, intraparietal sulcus. See also Figure S2.

(B) Conjunction analysis map. The map of the voxels significantly activated in both monkeys with Hit > CR contrast is shown (conjunction null, $p < 0.05$, corrected by FDR). Conventions are the same as in (A).

We also conducted effective connectivity analyses from retrieval-related areas in PPC, either PEa/DIP or PG/PGOp, to that in earlier visual areas (V4) (Figure S3). In the PPI analyses from the two PPC sites to V4 (Hit4 > Hit2), PEa/DIP showed a significantly positive PPI during a serial probe recognition task ($p < 0.001$, FWE corrected, small volume correction for V4), while PG/PGOp did not ($p > 0.05$, FWE corrected).

Cortical Network Modules of Retrieval-Related Regions

The above findings implied functional dissociation between IPL (PG/PGOp) and medial IPS (PEa/DIP). To further confirm this difference at the brain-wide network level, we first compared the anatomical connection maps of the two PPC sites, IPL (red, Figure 4A, left) and medial IPS (blue, Figure 4A, left). The overlap between these two anatomical connection maps was

Table 1. Brain Regions Activated in Hit > CR Contrast

Hemisphere	Coordinates (mm) x	y	z	t Value	Area	Module
Parietal Cortex						
L	−4	−26	8	5.62	23	2
L	−22	−20	16	4.15	PG/PGOp	2
R	21	−24	15	4.52		2
R	6	−18	16	3.91	PECg	2
L	−7	−25	13	6.33	PEa/DIP	3
R	6	−26	14	7.11		3
L	−10	−18	18	5.42	PEa	3
R	24	−10	5	4.41	PF/PFOp	4
L	−24	−9	10	4.13		4
L	−22	−3	11	5.26	2	4
Hippocampus						
L	−13	−12	−7	5.40	mHC	1
R	12	−20	−5	5.04	pHC	1
L	−15	−17	−5	4.05		1
Frontal Cortex						
R	11	10	14	5.81	8B	2
L	−16	3	6	3.52	44	3
L	−16	7	10	4.74	45B	3
R	11	8	6	4.21		3
R	16	12	9	5.05	9/46V	3
L	−6	−4	17	5.21	6/32	3
L	−3	3	19	4.32	6M	3
L	−23	2	11	5.29	6VR(F5)	4
R	20	3	8	5.79		4
Temporal Cortex						
L	−17	−7	−11	3.70	IPa	2
L	−22	−16	10	5.05	Tpt	2
R	20	−20	11	5.63		2
L	−22	2	−10	5.13	ST1	6
L	−25	−3	−2	3.51	ST3	4
Insular Cortex						
R	15	3	−3	3.45	AI	4
L	−19	2	−1	5.18	DI	4
R	21	1	1	4.71		4
Occipital Cortex						
R	10	−32	−3	4.28	V2	5
L	−12	−33	−3	5.16		5
R	10	−38	−3	5.11	V2	5
L	−16	−33	4	3.68	V2	5
R	2	−40	3	4.98	V2	5
R	7	−33	5	4.67	V2	5
L	−4	−35	8	3.93		5
L	−26	−24	5	4.61	V4	5
R	5	−28	6	4.71	PO	5
L	−18	−29	11	5.77	V4D	5
L	−14	−26	12	5.90	V4A	5
Subcortical						
L	−9	4	−2	3.93	AcbC	2
L	−9	−11	0	4.44	Thalamus	4
R	12	−8	5	3.83	Pu	4
L	−12	−2	10	5.09	Cd	4
R	6	−13	−5	4.78	SN	6
L	−14	−19	1	4.56	Cd	6

Significant peaks at a voxel level of $p < 0.01$ corrected by FDR. Coordinates are listed in monkey bicommissural space (Koyama et al., 2004; Nakahara et al., 2002). The abbreviations for the areas are provided in Table S1.

marginal. Next we calculated the functional connectivity map of spontaneous BOLD activity under anesthesia (Figure 4A, right). The functional connectivity map for seed regions of PG/PGOp (red, Figure 4A, right) covered the lateral parietal cortex and posterior cingulate cortex, while the map for PEa/DIP (blue, Figure 4A, right) covered the principal, arcuate, and intraparietal sulci. The overlap between these functional connectivity maps was also marginal. Moreover, the anatomical connection maps were in close agreement with functional connectivity maps. Then we evaluated the anatomical and functional connection patterns of the two PPC sites in whole brain (Figures 4B and S4A, see Supplemental Experimental Procedures) with the aid of CoCoMac database (collection of past tracer studies in the macaque cerebral cortex) (Stephan et al., 2001). As reported previously (Vincent et al., 2007), the strengths of anatomical connections were significantly correlated with the functional connectivities (PG/PGOp: $r = 0.45$; $p < 0.001$; PEa/DIP: $r = 0.42$, $p = 0.002$) (Figures S4C and S4D). From multiple regression analyses, functional connectivity with PG/PGOp is significantly correlated with the strength of axonal projections with PG/PGOp ($p < 0.001$) but not with PEa/DIP ($p > 0.05$) (Figure S4E, left panel). On the other hand, functional connectivity with PEa/DIP is significantly correlated with the strength of axonal projections with PEa/DIP ($p < 0.001$) but not with PG/PGOp ($p > 0.05$) (Figure S4F, right panel). These results suggested that the anatomical connection patterns of the two PPC sites are dissociated enough to separately predict functional connectivity with the two PPC sites, respectively (Figures S4C, S4D, and S4E). In addition, we compared the anatomical connection (Figure S4F) and functional connectivities (Figure S4G) for all combinations of retrieval-related areas. The strengths of anatomical connections were again significantly correlated with the functional connectivity ($r = 0.23$; $p = 0.003$) (Figure S4H).

To objectively segregate the 47 identified retrieval-related regions including PG/PGOp and PEa/DIP, we conducted community detection analysis using modularity optimization of the functional connectivity of spontaneous BOLD activity under anesthesia from the same monkeys as the recognition memory experiments (Rubinov and Sporns, 2011) (see Supplemental Experimental Procedures). We configured a matrix of pairwise functional connectivity correlations between each of the 47

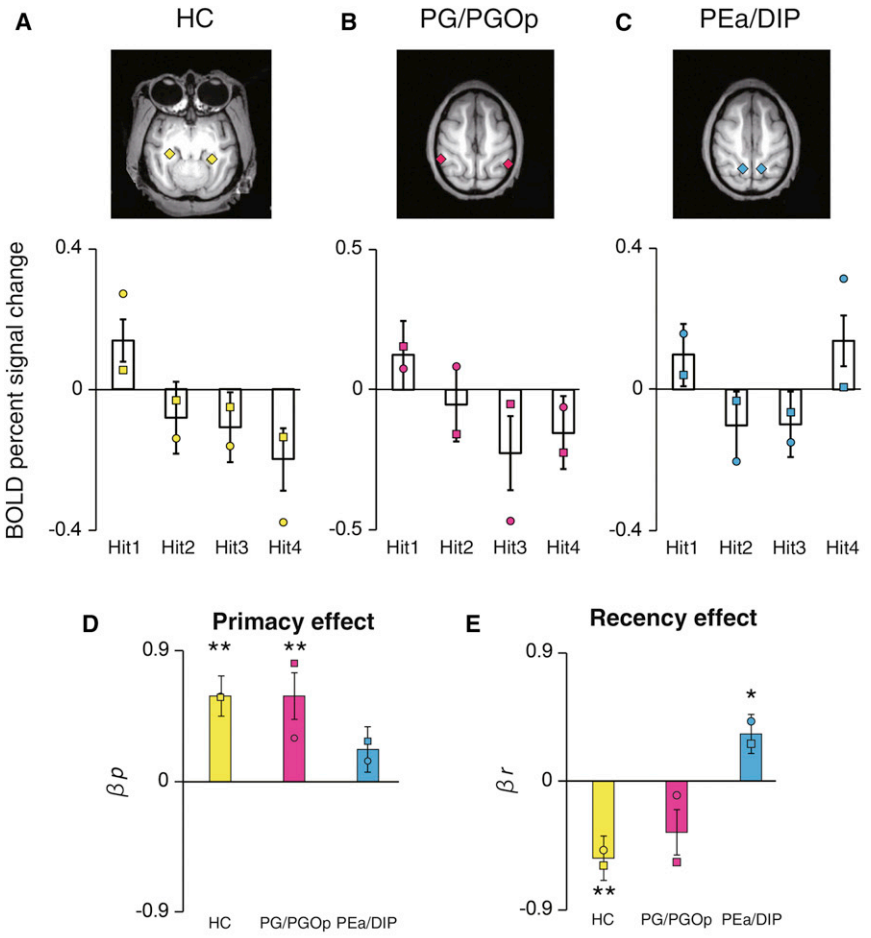

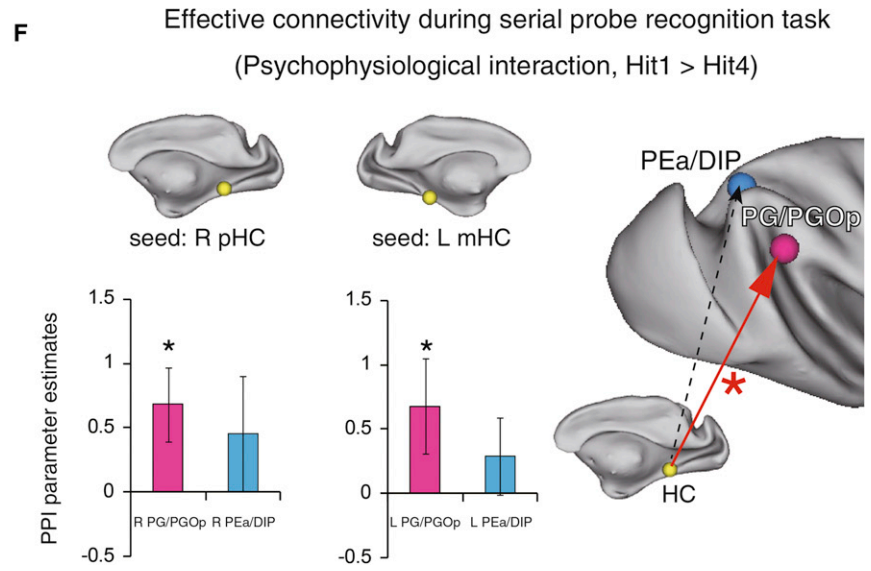

Figure 3. BOLD Signal Changes and Task-Evoked Connectivity during Retrieval in the Serial Probe Recognition Task

(A–C) BOLD percent signal changes in the Hit trials compared with those in the CR trials (Hit versus CR). Abscissa, four types of Hit trials (Hit1–Hit4) classified according to retrieved cue item position. (A) hippocampus (HC; right pHC and left mHC). (B) Posterior inferior parietal lobule (bilateral PG/PGOp). (C) Intraparietal sulcus (bilateral PEa/DIP). Each square and circle represents the average signal change from monkey A and monkey V, respectively. Error bars: SEM.

(D and E) Comparisons of β coefficient calculated by regression analyses. Abscissa, three regions in (A) to (C). (D) β coefficient for primacy effect (β_p). (E) β coefficient for recency effect (β_r). *$p < 0.05$, **$p < 0.01$ with Bonferroni correction. Each square and circle represents the β coefficient for monkey A and monkey V, respectively. Error bars: SEM.

(F) Psychophysiological interactions (PPI) in the serial probe recognition task. The left panel shows the couplings between the right posterior hippocampus (pHC) and the two PPC subregions (right PG/PGOp and right PEa/DIP) in retrieval of the initial item (Hit1) after subtraction of those in retrieval of the last item (Hit4). The asterisks indicate significant increase in effective connectivity ($p < 0.05$, FWE corrected within each region). Error bars: SEM. Middle panel shows the results of PPI analysis of effective connectivity from the left middle hippocampus (mHC) to the left PG/PGOp and left PEa/DIP. The right panel shows a scheme of effective connectivity from hippocampus to parietal regions (PG/PGOp, PEa/DIP). Red arrow with asterisk: significant positive effective connectivity. Black dotted arrow: nonsignificant effective connectivity. See also Figure S3.

regions (Figure 4C). Modularity optimization separated the regions into six distinct groups, or modules (modularity measure Q = 0.59), where PG/PGOp and PEa/DIP were classified separately. This Q value indicated strong community structure that exceeded the criterion adopted by previous studies, 0.30 (Nelson et al., 2010; Newman, 2006). Module 1 consisted of bilateral hippocampi. Module 2 (pink, Figure 4E) contained bilateral PG/PGOp, temporo-parietal areas (Tpt), posterior cingulate cortices (area 23, PECg), and right area 8B. These regions were included among the areas that demonstrated high functional connectivity to the seed region of PG/PGOp (red, Figure 4A). Module 3 (light blue, Figure 4E) contained bilateral PEa/DIP, area 45B, and right area 9/46V. These regions were included among the areas that demonstrated high functional connectivity to the seed region of PEa/DIP (blue, Figure 4A). These results confirmed that the two parietal retrieval-related regions, PG/PGOp and PEa/DIP, are involved in separate retrieval-related networks. Module 4 (orange, Figure 4E) contained bilateral

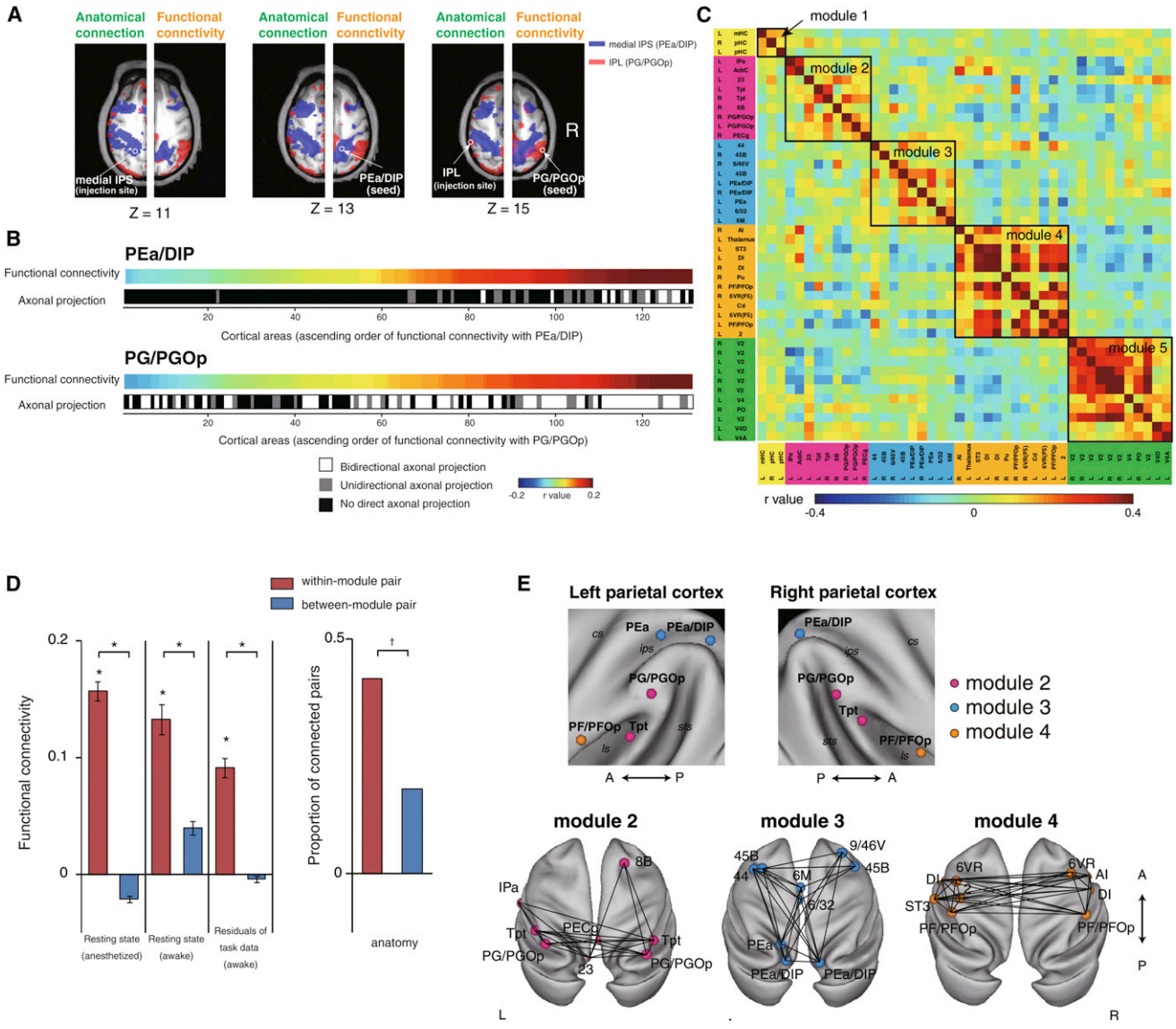

Figure 4. Five Modules of Retrieval Network Identified by Modularity Optimization

(A) Anatomical connection and functional connectivity maps. Left half in each panel: anatomical connection maps obtained from the data of tracer injection in Lewis and Van Essen (2000). Small circles indicate the location of injection sites (IPL, red, case D; medial IPS, blue, case A). Right half in each panel: voxel-wise map of spontaneous BOLD functional connectivity (BOLD-FC) obtained with the seed regions at the right PG/PGOp (red) and at the right PEa/DIP (blue). Small circles indicate the location of seed regions. Maps are thresholded at $r > 0.12$.

(B) Anatomical and functional connection patterns of PEa/DIP and PG/PGOp in whole brain. Anatomical connections of the listed 131 areas with either PEa or PG have been described in the previous literature in the CoCoMac database. These areas are arranged in ascending order of functional connectivity. The area names are provided in Figure S4A. In the rows of "Axonal projection," a white bar indicates the presence of bidirectional axonal connection, a gray bar indicates the presence of unidirectional axonal connection, and a black bar indicates the absence of confirmed axonal connection.

(C) BOLD-FC matrix among the retrieval-related regions listed in Table 1. Rows and columns indicate the regions sorted by optimized modules. Retrieval-related regions were split into nonoverlapping modules, one of which (module 1 [yellow]) consisted of hippocampus, three of which (module 2 [pink], module 3 [light blue], module 4 [orange]) contained regions within the PPC, and one of which (module 5 [green]) consisted of regions in the occipital cortex.

(D) Left panels: comparisons of functional connectivity between within- (red) and between-module (blue) pair of retrieval-related areas from the data of the resting state experiment of the anesthetized monkeys (left), the data of the resting state experiment of the awake monkeys (middle), and the data from the analysis of residual time courses of the awake task experiment (right). *: $p < 0.001$. Error bars: SEM. Right panel: comparisons of proportion of anatomically connected pairs between within- and between-module pair of retrieval-related areas. †: $p < 0.001$ (chi-square test).

(E) Spatial configurations of the retrieval-related modules in the macaque cortex. Modules are displayed on the inflated cortical surface using Caret software. Upper panels show module assignments in PPC. cs, central sulcus; ips, intraparietal sulcus; ls, lateral sulcus; sts, superior temporal sulcus. Lower panels show all the cortical regions in the three modules containing PPC regions (module 2, 3, 4). Pairs of regions in each module with significant BOLD-FC are interconnected with lines ($p < 0.05$, Bonferroni correction by the number of combinations among all the retrieval-related regions). See also Figure S4.

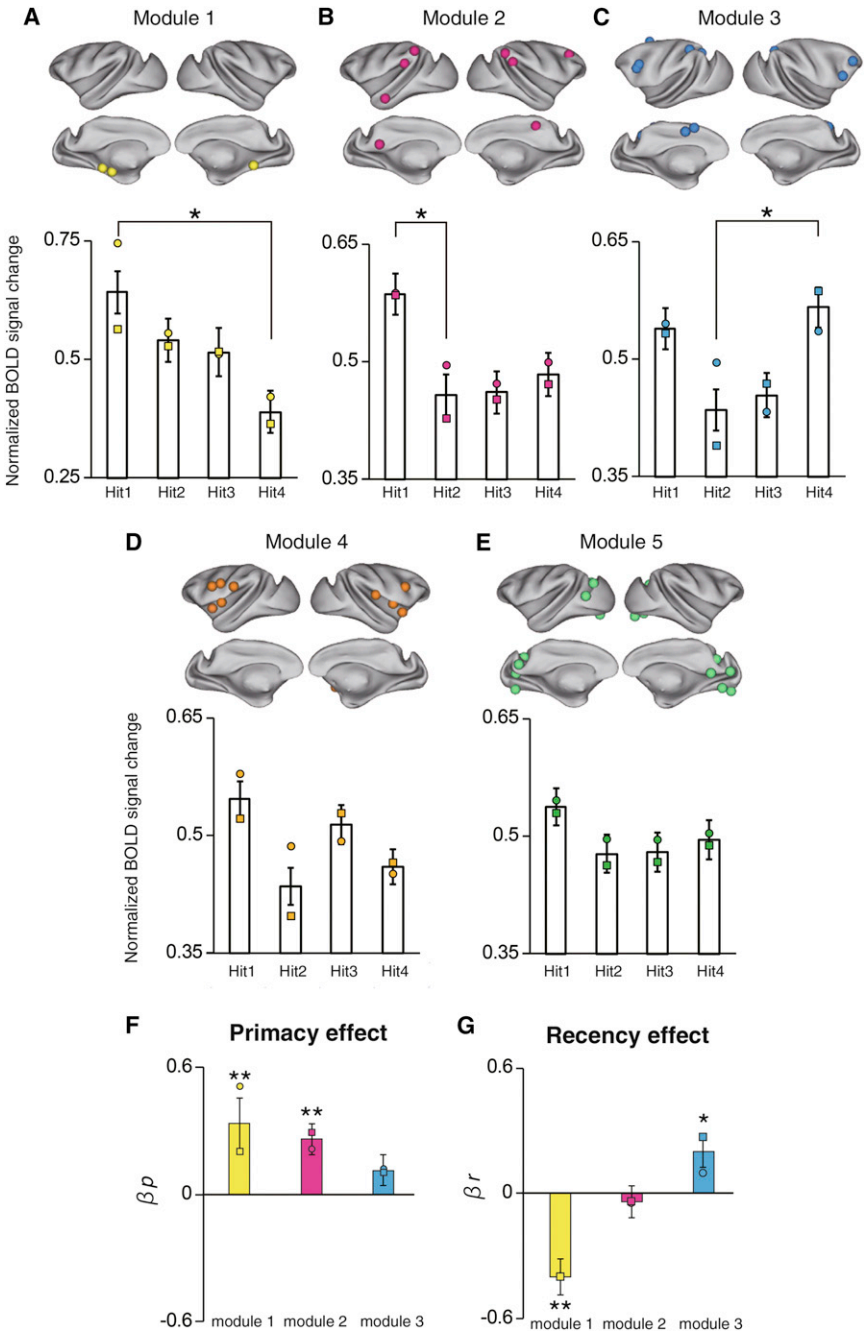

Figure 5. Primacy Effect and Recency Effect in Retrieval Network Modules

(A) Retrieval-related activity within module 1. Abscissa: the four types of Hit trials (Hit1–Hit4) classified by the retrieved cue item position. Ordinate: Normalized percent signal changes of all the constituent retrieval-related regions in this module. Each square and circle represents the average signal change from monkey A and monkey V, respectively. *: $p < 0.05$ (paired t test, Bonferroni corrected). Error bars: SEM. All the regions in module 1 are shown on lateral and medial views of the cortex using Caret software.

(B–E) Same as in (A) but for module 2 (B), module 3 (C), module 4 (D), and module 5 (E).

(F and G) Comparisons of β coefficient calculated by regression analyses. Abscissa, three modules shown significant main effect of the retrieved cue item position in MANOVA (module 1, 2, 3). (F) β coefficient for primacy effect (β_p). (G) β coefficient for recency effect (β_r). *: $p < 0.05$, **: $p < 0.01$ with Bonferroni correction. Each square and circle represents the β coefficient for monkey A and monkey V, respectively. Error bars: SEM. See also Figure S5.

6VR, insula, and anterior IPL (PF/PFOp). Module 5 covered all regions in occipital cortex. Module 6 was excluded from later analysis because two of the three regions belonged to subcortical areas. The fact that retrieval-related regions in PPC participated in three (modules 2, 3, 4) of the six modules (Figure 4E, upper panel) suggests that the different modules of a brain-wide memory-retrieval network coexist in PPC.

Resting state data in the awake condition was also collected from the same two monkeys (Figure S4B). We confirmed that the modular structure extracted from spontaneous BOLD activity in anesthetized monkeys was preserved in awake monkeys ($p < 0.001$ for each) (Figure 4D, left panels). We also confirmed that the proportion of anatomically connected pairs of areas within the same module was significantly higher than pairs from different modules ($p < 0.001$) (Figure 4D, right panel). Thus, the modular structures extracted from the functional connectivity networks reflected the anatomical structures of the retrieval-related networks.

Cortical Network Reflecting the Primacy and Recency Effects

Finally, we examined whether population activity within each of the separated modules above reflects the primacy or recency effects. For module 1, MANOVA (four levels of retrieved cue item positions × regions within the module × two monkeys) yielded a significant main effect of retrieved cue item position ($F(3,22) = 3.67$, $p = 0.02$) on normalized BOLD signals (see Experimental Procedures) with no interactions with the level of region ($F(6,19) = 1.91$, $p = 0.13$) or monkey ($F(3,22) = 0.46$, $p > 0.5$) (Figure 5A). For module 2, MANOVA yielded a significant main effect of retrieved cue item position ($F(3,22) = 3.80$, $p = 0.02$) with no interactions with the level of region ($F(24,1) = 0.30$, $p > 0.5$) or monkey ($F(3,22) = 0.20$, $p > 0.5$) (Figure 5B). For module 3, MANOVA yielded a significant main effect of retrieved cue item position ($F(3,22) = 4.37$, $p = 0.01$) with no interactions with the level of region ($F(24,1) = 0.24$, $p > 0.5$) or monkey ($F(3,22) = 1.62$, $p = 0.21$) (Figure 5C). Modules 4 and 5 did not demonstrate any significant main

effects of retrieved cue item position (all $p > 0.05$) (Figures 5D and 5E).

For modules 1 to 3, which demonstrated a main effect of retrieved cue item position, we conducted regression analyses using a "primacy predictor" (n_p) and "recency predictor" (n_r) for the normalized BOLD signal from Hit1 to Hit4. Module 1 demonstrated significant positive modulation by retrieval of the initial items ($\beta_p = 0.33 \pm 0.12$, $t(77) = 2.80$, $p = 0.01$) with significant negative modulation by retrieval of the last items ($\beta_r = -0.39 \pm 0.12$, $t(77) = -3.05$, $p = 0.006$) (Figures 5A, 5F, and 5G). Module 2 demonstrated positive modulation by retrieval of the initial items ($\beta_p = 0.26 \pm 0.07$, $t(233) = 3.64$, $p < 0.001$) but no significant modulation by retrieval of the last items ($\beta_r = 0.03 \pm 0.07$, $t(233) = -0.51$, $p > 0.5$) (Figures 5B, 5F, and 5G). Conversely, module 3 demonstrated significant positive modulation by retrieval of the last items ($\beta_r = 0.19 \pm 0.07$, $t(233) = 2.79$, $p = 0.01$) with no significant modulation by retrieval of the initial items ($\beta_p = 0.11 \pm 0.07$, $t(233) = 1.58$, $p = 0.22$) (Figure 5C, 5F, and 5G). In summary, the MANOVA and the regression analyses applied here indicate that modules 1 and 2 are involved in retrieval of the initial cue items, which is related to primacy effect, module 3 is involved in retrieval of the last items, which is related to recency effect, and modules 4 and 5 are not affected by retrieved cue item position. Post hoc multiple comparisons between each pair of cue item positions also confirmed these findings: module 1 was more activated by retrievals of the first item than the last (Hit1 > Hit4, $p = 0.01$, Bonferroni correction; other pairs $p > 0.05$), module 2 was more activated by the first item than the second (Hit1 > Hit2, $p = 0.03$, Bonferroni correction; other pairs $p > 0.05$), and module 3 was more activated by the last item than the second (Hit4 > Hit2, $p = 0.01$, Bonferroni correction; other pairs $p > 0.05$). These results demonstrated that the segregated modules of the retrieval-related network showed differential response characteristics in the retrieval of different cue item positions.

Retrieval activities for error trials (FA and miss) as well as correct trials (hit and CR) were also compared among modules in the single-probe recognition task (Figure S5). Each module showed differential response characteristics in two distinct comparisons, FA versus CR and Hit versus Miss. These results suggested that the modules would also differentially reflect various task components other than primacy or recency effects (see Supplemental Text).

DISCUSSION

This study is the first demonstration of awake monkey fMRI experiments during recognition memory retrieval. In the present study, we first identified retrieval-related regions that were active for correct recognition of seen items compared to correct rejection of unseen items (old/new effect). We then found functional dissociation of the monkey retrieval-related regions in PPC, PG/PGOp in IPL and PEa/DIP in IPS, based on the serial position effect. Finally, network analyses for the functional connectivity of task-evoked and spontaneous BOLD activity confirmed that PEa/DIP and PG/PGOp were separately embedded in different brain-wide subnetworks of the retrieval-related regions, and these two subnetworks were also differently characterized by the serial position effect.

In the serial probe recognition task, a typical U-shaped serial position curve of corrected recognition rate accompanied by primacy and recency effects was observed in both monkeys (Figure 1). Human studies have attributed the primacy effect to facility in retrieving the first item that is consolidated in long-term memory during the encoding process (Atkinson and Shiffrin, 1968). A recent behavioral study suggested that long-term memory processes also elicited the primacy effect in monkeys (Basile and Hampton, 2010). The retrieval-related activity reflecting the primacy effect in the present study (Figures 3A and 3B) would contribute to long-term episodic memory retrieval in monkeys. It is unlikely that the activities reflect general task demands because these activities were not observed in the trials with recency effect. Indeed, among the retrieval-related regions, bilateral hippocampi reflected the primacy effect. This modulation of hippocampal activity is consistent with the previous report in humans that specific impairment of the primacy effect but no impairment of recency effect are followed by damage to bilateral hippocampi (Baddeley and Warrington, 1970). Thus, hippocampal activity identified in this study is suggested to be related to long-term memory retrieval.

In the parietal cortex, we found retrieval-related activity in the posterior IPL (PG/PGOp) and the IPS (PEa/DIP) (Figure 2; Table 1). These macaque parietal areas have long been considered multimodal processing areas where information from somatosensory and visual cortices is integrated (Andersen and Buneo, 2002; Bisley and Goldberg, 2010). In the present study, contribution of macaque PPC to recognition memory retrieval was revealed for the first time. In addition, the retrieval-related activities in PG/PGOp and PEa/DIP were dissociated with respect to both response profiles for retrieved cue item positions and effective connectivity with the hippocampus. Anatomically, PG/PGOp is known to receive disynaptic input from the CA1 region of the hippocampus via the parahippocampal gyrus (Clower et al., 2001). By contrast, PEa/DIP is known to receive input from adjacent areas including PO, the ventral lateral intraparietal area (POal), and dorsal area 5 (PEC) (Lewis and Van Essen, 2000), while anatomical connections with hippocampus or parahippocampal gyrus have not been determined. This closer anatomical relationship of hippocampus with PG/PGOp than with PEa/DIP might mediate the enhancement of effective connectivity for the requirement of long-term memory retrieval. In humans, the angular gyrus (Brodmann area 39) in the posterior IPL, which shows the "old/new effect" in memory retrieval, is known to functionally connect with hippocampus (Vincent et al., 2006), and in addition, both angular gyrus and hippocampus demonstrated increased activity during successful episodic retrieval of long-term memory (Huijbers et al., 2010; Yonelinas et al., 2005). The identified retrieval-related area in macaque PG/PGOp, which was more highly activated and more strongly connected with hippocampus when retrieval from long-term memory was required, is thus implied to functionally correspond to the human angular gyrus in memory retrieval.

While primacy-effect related activities were identified in IPL (PG/PGOp), recency-effect related activities were identified in

IPS (PEa/DIP). Electrophysiological studies of macaque DIP neurons (Nieder, 2005) reported neuronal activity involved in memorizing sequences of events (numbers), which was further investigated in theoretical studies (Botvinick and Watanabe, 2007). These sequence-selective activities of IPS neurons might partially account for the fMRI activity profile of PEa/DIP in the present study but do not explain our observation that PEa/DIP activity was selective only to the last item retrieval (Figure 3C). Further examinations of the fMRI activity spots in cellular level will clarify the neuronal basis of the differentiation between IPS and IPL regarding the retrieval of items in a sequence.

In the frontal cortex, we identified retrieval-related activity in bilateral dorsolateral (area 9/46V) and ventrolateral (area 45) prefrontal areas (Figure 2; Table 1). In previous human studies, specific areas within dorso- and ventrolateral prefrontal cortices are active for the correct recognition of seen items, and are suggested to play differential roles in the selection of memory representation and postretrieval monitoring during both episodic and working memory processes (for reviews see Cabeza and Nyberg, 2000; Petrides, 2005). The tendency of these frontal regions to be active for retrieval of the last items in this study (Figure 5C) reflects their responsibility for the retrieval of recently encoded items, which might be actively maintained in the working memory. It will be of great interest to study how these frontal areas work cooperatively with PEa/DIP during retrieval from working memory.

Recently, the role of the PPC has been associated with top-down and bottom-up attention during memory processes in humans (Cabeza et al., 2008; Corbetta and Shulman 2002; Vilberg and Rugg, 2008). Ventral PPC is thought to be involved in reorienting attention to memory via "bottom-up" pathways, while dorsal PPC is thought to be involved in reorienting attention to memory via "top-down" pathways in humans. In the present study, the PPI analyses (Figures 3F and S3) showed contrasting results between the two macaque PPC areas, which suggest bottom-up attention from the hippocampus to the IPL (Figure 3F) and top-down attention from the IPS to V4 (Figure S3). These results were consistent with this model of human PPC functions.

Analysis of spontaneous BOLD activity revealed that functional dissociation within the macaque PPC was accompanied by network-level dissociation (Figures 4E, 5B, and 5C). Human studies have shown that each of functional networks identified from spontaneous BOLD activity matches a set of brain regions that cooperate during active cognitive tasks (Smith et al., 2009). In the present monkey study, the two retrieval-related areas in PPC, PG/PGOp, and PEa/DIP, were embedded in distinct subgroups: the former was functionally connected with the superior branch of arcuate sulcus (area 8B), posterior cingulate cortex (area 23, PECg), and temporoparietal areas (Tpt) (module 2, pink, Figure 4E), while the latter was mainly connected with the lateral prefrontal cortex (area 45B, 9/46V) (module 3, light blue, Figure 4E). The areas included in module 2 (area 23, PECg [PEci], IPa, and Tpt) exhibited anatomical connection with PG (PG-injection cases, 20, 27, and 29 in Rozzi et al., 2006). The dependency of the retrieval-related activity on retrieved item position differed between these modules: module 2 including PG/PGOp reflected the primacy effect, while module 3 including PEa/DIP reflected the recency effect. Module 2 was included in the functional connectivity map for the seed of posterior cingulate/precuneus cortex, which is known as the "default-mode network" of monkeys (Mantini et al., 2011; Vincent et al., 2007). Area 8B and area 23 in module 2 are especially known to reduce its activity during performance of goal-directed tasks (Mantini et al., 2011). In humans, the default-mode network is associated with episodic memory function (Vincent et al., 2006). The angular gyrus, which is activated during episodic memory retrieval, is included in the network, and is suggested to act as one of the hubs (Nelson et al., 2010). Their participation in the default-mode network will provide additional evidence for the functional correspondence between the macaque PG/PGOp and human angular gyrus. Meanwhile, module 3 was included in the frontoparietal network (for humans, Corbetta and Shulman, 2002; for monkeys, Hutchison et al., 2011; Vincent et al., 2007). In humans, this network is considered to be related to top-down attention (Corbetta and Shulman, 2002). The human intraparietal regions, which are activated during working memory retrieval and mediate memory control processes, are included in the network (Nelson et al., 2010; Vilberg and Rugg, 2008). This interspecies correspondence in terms of the cognitive role and functional connectivity with the frontal cortex suggests that the human counterpart of macaque PEa/DIP resides in the human intraparietal regions. Further work will establish the functional correspondence between retrieval-related PPC in humans and macaques.

In the present study, the brain regions involved in primacy and recency effects were represented not only in the level of specific brain regions but also in the level of modules, each of which consists of functionally connected areas. This network-level dissociation suggested that the primacy and recency effects reflected two distinct memory processes (Baddeley and Warrington, 1970, Talmi et al., 2005) and would not be explained by a single mechanism based on relative temporal distinctiveness or on context variability. However, serial position effect is complex and actually influenced by various cognitive processes depending on task conditions. In humans, differential activity profiles of dorsal and ventral PPC were shown as a function of retrieval delay (Huijbers et al., 2010), but the profiles were varied depending on task (Talmi et al., 2005). Therefore, to establish the monkey counterparts of the human retrieval success areas that were typically identified in long-term memory paradigms, it is needed to examine further primacy effect-related activity in other task conditions which require long-term memory processes.

In this study, we combined fMRI activation analysis and connectivity analyses based on task-evoked and spontaneous BOLD activities. All these analyses converged to reveal the functional dissociation within PPC during memory retrieval in monkeys. The multimodal approach in combination with connectivity-based methods is useful to characterize and classify brain regions cooperatively interacting for specific functions. Furthermore, network-level analysis in monkeys whose anatomical structure is well known will provide important clues to understanding the relationship between functionally identified networks and structural anatomical networks at a level unattainable with experimentation in humans.

EXPERIMENTAL PROCEDURES

Subjects and Behavioral Tasks

All the experimental protocols were in full compliance with the regulations of the University of Tokyo School of Medicine and with the NIH guidelines for the care and use of laboratory animals. Two adult monkeys (*Macaca fuscata*) participated in the experiment. fMRI experiments were conducted as described previously (Koyama et al., 2004; Nakahara et al., 2002). Online behavioral control and reward delivery were implemented in the Presentation platform as described previously (Kamigaki et al., 2009; see Supplemental Experimental Procedures for details).

The monkeys performed a serial probe recognition task (Wright et al., 1985) modified for fMRI (Figure 1A). Each trial began with the presentation of a fixation point after the monkey pulled the joystick ("Warning," Figure 1A). The list items then appeared serially ("Cue 1–4"). Each item was presented at the center of the monitor for 1 s followed by interstimulus intervals of 1 s. The items were selected from the 1,000-picture pool in a pseudorandom order. Typically, each picture was presented in only one trial (two trials at most) in each session. The last list item was followed by a delay period variably changed trial-by-trial between 7 and 10 s ("Delay"). Finally, the monkey was presented with one test item at the center and two symbols, a triangle and a cross, on the left and right sides of the image ("Choice"). The assignment of symbols to the left or right side was randomly selected trial by trial. In half the trials, the item in the choice period was the same as one of the cue items, and in the other half of trials, the item had not been presented as a cue item. Monkeys responded by moving the joystick in the "seen" symbol direction (a triangle for monkey A and a cross for monkey V) if the test item was from the cue item list, or by moving the joystick in the "unseen" symbol direction (a cross for monkey A and a triangle for monkey V) if it was not from the list. The monkey received juice drops, accompanied by a distinctive secondary visual reinforcement ("Feedback"). Incorrect choices resulted in termination of the trial without reward. Trials were separated by a 4 s intertrial interval, during which the screen was black. If any limbs moved during the trials, the optic sensors detected the movement and the trial was aborted immediately. At the first stage of experiments, which lasted for 24–26 sessions, the monkeys performed a single-probe recognition task (number of cue items = 1) to localize retrieval-related regions (Figure S1A). The task procedure was the same as above but used a single item for the cue. The monkeys then performed the serial probe recognition task (number of cue items = 4).

Data Acquisition

Functional images were acquired in a 4.7-T MRI scanner (Biospec 47/40, Bruker, Ettlingen) with 100 mT/m actively shielded gradient coils and a transceiver saddle RF coil (Takashima, Tokyo) (Adachi et al., 2012; Koyano et al., 2011; Matsui et al., 2007, 2011, 2012). In each session, functional data were acquired using a gradient-echo echo-planar imaging (EPI) sequence (1-shot, TR = 2.5 s, TE = 20 ms, 1.25 × 1.5 mm^2 in-plane resolution, 64 × 96 matrix, slice thickness = 1.5 mm with inter-slice gap = 0.25 mm, 27 horizontal slices covering the whole brain). To assess spontaneous functional connectivity between the retrieval-related regions detected in the above fMRI sessions, fMRI data under anesthesia were collected (Adachi et al., 2012; Matsui et al., 2011; Vincent et al., 2007) from the same monkeys used for the recognition memory experiments. During the acquisition of functional images, anesthesia was maintained with continuous intravenous infusion of dexmedetomidine (10–15 μg/kg/hr). Resting-state data in awake condition was also collected from the same monkeys used for the recognition memory experiments. During the acquisition of functional images, the movements of each of the four limbs were monitored. The monkeys were rewarded as long as all limbs stay motionless at intervals of 3–5 s.

Identification of Retrieval-Related Regions

To localize retrieval-related regions, the data from the single-probe recognition task were preprocessed with SPM5 (http://www.fil.ion.ucl.ac.uk/spm). Functional images were realigned, corrected for slice timing, spatially normalized to the template image with interpolation to a 1 × 1 × 1 mm^3 space, and smoothed with a Gaussian kernel (3 mm full-width at half-maximum [FWHM]). The template image was constructed from the high-resolution EPI of monkey A by coregistering it to monkey A's anatomical template MDEFT image arranged in bicommissural space in which the origin was placed at the anterior commissure (Koyama et al., 2004; Nakahara et al., 2002).

The retrieval-related regions were identified by performing voxel-wise GLM analyses implemented in SPM5. These analyses included the following predictors: (1–4) the choice onsets in Hit, CR, Miss, and FA trials; (5–9) the cue onsets in Hit, CR, Miss, FA, and other (aborted) trials; and (10) the timing of other types of errors. These events were modeled as delta functions convolved with the canonical hemodynamic response function and its temporal and dispersion derivatives. The six parameters of head motion derived from realignment were also included in the model as covariates of no interest. Data were high-pass filtered using a cutoff of 32 s. The group analysis of the data from the two monkeys was conducted by using a fixed-effect model. Retrieval-related regions were identified as the group analysis map (Figure 2A) of the comparison of BOLD signals between the Hit and CR conditions (Konishi et al., 2000). The coordinates of the activation peaks at which the t value was significant at $p < 0.01$ with FDR correction (Genovese et al., 2002) were included in Table 1. These peaks were labeled by referring to the atlas of Paxinos et al. (2008). For the two PPC areas, PG/PGOp and PEa/DIP, we confirmed the locations of peaks with coordinate registrations in Caret software (Nelissen et al., 2011; Peeters et al., 2009; see Supplemental Text for details). To examine the reproducibility of the results from two monkeys, a conjunction map (conjunction null, $p < 0.05$, FDR corrected) of retrieval-related regions was generated (Friston et al., 2005; Nichols et al., 2005).

Retrieval Activity and Task-Evoked Connectivity Reflecting Serial Position Effects

Voxel-wise GLM analyses were conducted for functional images acquired in experiments using the serial probe recognition task after preprocessing. Hit and Miss trials were further classified respectively into four categories according to the item position in the cue sequence in which the tested image in the choice period was presented (Hit1–4 and Miss1–4). The retrieval activities in the serial probe recognition task were measured in each ROI defined in Table 1 using the MarsBaR ROI toolbox for SPM. To examine the effect of cue item position on the retrieval-related activities in each homotopic pair of ROIs in the hippocampus and posterior parietal cortex (left mHC and right pHC; bilateral PG/PGOp; bilateral PEa/DIP) (for the criteria to select these areas, see Supplemental Text), an across-session repeated-measures MANOVA of the percentage of BOLD signal changes at each of the choice onsets of Hit1–4 trials was conducted. Then, we conducted regression analyses (Figures 3D and 3E; see Supplemental Experimental Procedures for details) to assess the activity enhancement of each ROI in the retrieval of the initial and last items in the cue sequence (primacy effect-related and recency effect-related activity, respectively).

To examine the effect of item positions in the cue sequence on effective connectivity between the hippocampus and the two posterior parietal retrieval-related regions (PG/PGOp, PEa/DIP), PPI analyses were conducted for the serial probe recognition task using SPM5. The effect size of the PPI at the two parietal regions with the seed at the hippocampus was evaluated as the beta estimate for the PPI predictor averaged across all sessions from the two monkeys, and the statistical threshold was set at $p < 0.05$ (FWE corrected within each region).

Group Classifications of Retrieval-Related Regions Based on Functional Connectivity

In addition to standard preprocessing steps as described above for task-based fMRI, functional images of spontaneous activity under anesthesia underwent several additional preprocessing steps for intrinsic correlation analyses, as described previously (Adachi et al., 2012; Fox et al., 2005; Matsui et al., 2011). Graph theory-based analyses on the functional connectivity matrix (Figure 4C) were performed to test whether distinct groups or "modules" existed within the network of functional connectivity among the retrieval-related regions, which might provide further distinctions between the ROIs of the retrieval-related regions (Newman, 2006; see Supplemental Experimental Procedures for details). For each of the detected modules of the retrieval-related areas, whether modulation of the gross retrieval activity

within the module depended on the item positions in the cue sequence was examined by conducting a repeated-measures MANOVA (four levels of retrieved cue item positions × regions within the module × two monkeys) for the signal changes at the choice onsets of Hit1–4 trials from all the ROIs comprising the module. For this analysis, the percent signal changes of each ROI were normalized to eliminate the variability of the signal across sessions from two monkeys (see Supplemental Experimental Procedures). For modules that showed a significant main effect of retrieved cue item position without significant interaction with monkey or ROI in the MANOVA, we further conducted regression analyses to evaluate primacy effect-related and recency effect-related activities of these modules (Figures 5F and 5G; Supplemental Experimental Procedures).

SUPPLEMENTAL INFORMATION

Supplemental Information includes five figures, one table, Supplemental Experimental Procedures, and Supplemental Text and can be found with this article online at http://dx.doi.org/10.1016/j.neuron.2012.12.019.

ACKNOWLEDGMENTS

This work was supported in part by MEXT/JSPS KAKENHI Grant Numbers 19002010 and 24220008 to Y.M., by CREST, Japan Science and Technology Agency to Y.M., by a grant from Takeda Science Foundation to Y.M., and by Japan Society for the Promotion of Science Research Fellowships for Young Scientists to K.M. (234682) and T.M. (201204982). One Japanese monkey used in this research was provided by NBRP "Japanese Monkeys" through the National BioResource Project of the MEXT. We thank Tomomi Watanabe for technical assistance and Seiki Konishi and Takamitsu Watanabe for helpful comments on the manuscript.

Accepted: December 12, 2012
Published: February 20, 2013

REFERENCES

Adachi, Y., Osada, T., Sporns, O., Watanabe, T., Matsui, T., Miyamoto, K., and Miyashita, Y. (2012). Functional connectivity between anatomically unconnected areas is shaped by collective network-level effects in the macaque cortex. Cereb. Cortex *22*, 1586–1592.

Andersen, R.A., and Buneo, C.A. (2002). Intentional maps in posterior parietal cortex. Annu. Rev. Neurosci. *25*, 189–220.

Atkinson, R.C., and Shiffrin, R.M. (1968). Human memory: a proposed system and its control processes. In Psychology of Learning and Motivation, W.S. Kenneth and S.J. Taylor, eds. (San Diego: Academic Press), pp. 89–195.

Baddeley, A.D., and Warrington, E.K. (1970). Amnesia and the distinction between long- and short-term memory. J. Verbal Learn. Verbal Behav. *9*, 176–189.

Baldo, J.V., and Shimamura, A. (2002). Frontal lobes and memory. In Handbook of Memory Disorders, A.D. Baddeley, M.D. Kopelman, and B.A. Wilson, eds. (New York: John Wiley & Sons), pp. 363–379.

Basile, B.M., and Hampton, R.R. (2010). Rhesus monkeys (Macaca mulatta) show robust primacy and recency in memory for lists from small, but not large, image sets. Behav. Processes *83*, 183–190.

Bisley, J.W., and Goldberg, M.E. (2010). Attention, intention, and priority in the parietal lobe. Annu. Rev. Neurosci. *33*, 1–21.

Botvinick, M., and Watanabe, T. (2007). From numerosity to ordinal rank: a gain-field model of serial order representation in cortical working memory. J. Neurosci. *27*, 8636–8642.

Cabeza, R., and Nyberg, L. (2000). Imaging cognition II: An empirical review of 275 PET and fMRI studies. J. Cogn. Neurosci. *12*, 1–47.

Cabeza, R., Ciaramelli, E., Olson, I.R., and Moscovitch, M. (2008). The parietal cortex and episodic memory: an attentional account. Nat. Rev. Neurosci. *9*, 613–625.

Clower, D.M., West, R.A., Lynch, J.C., and Strick, P.L. (2001). The inferior parietal lobule is the target of output from the superior colliculus, hippocampus, and cerebellum. J. Neurosci. *21*, 6283–6291.

Corbetta, M., and Shulman, G.L. (2002). Control of goal-directed and stimulus-driven attention in the brain. Nat. Rev. Neurosci. *3*, 201–215.

Curtis, C.E., and D'Esposito, M. (2003). Persistent activity in the prefrontal cortex during working memory. Trends Cogn. Sci. *7*, 415–423.

Davidson, P.S.R., Anaki, D., Ciaramelli, E., Cohn, M., Kim, A.S.N., Murphy, K.J., Troyer, A.K., Moscovitch, M., and Levine, B. (2008). Does lateral parietal cortex support episodic memory? Evidence from focal lesion patients. Neuropsychologia *46*, 1743–1755.

Eichenbaum, H., Yonelinas, A.P., and Ranganath, C. (2007). The medial temporal lobe and recognition memory. Annu. Rev. Neurosci. *30*, 123–152.

Fox, M.D., Snyder, A.Z., Vincent, J.L., Corbetta, M., Van Essen, D.C., and Raichle, M.E. (2005). The human brain is intrinsically organized into dynamic, anticorrelated functional networks. Proc. Natl. Acad. Sci. USA *102*, 9673–9678.

Friston, K.J., Penny, W.D., and Glaser, D.E. (2005). Conjunction revisited. Neuroimage *25*, 661–667.

Genovese, C.R., Lazar, N.A., and Nichols, T. (2002). Thresholding of statistical maps in functional neuroimaging using the false discovery rate. Neuroimage *15*, 870–878.

Huijbers, W., Pennartz, C.M.A., and Daselaar, S.M. (2010). Dissociating the "retrieval success" regions of the brain: effects of retrieval delay. Neuropsychologia *48*, 491–497.

Husain, M., and Nachev, P. (2007). Space and the parietal cortex. Trends Cogn. Sci. *11*, 30–36.

Hutchison, R.M., Leung, L.S., Mirsattari, S.M., Gati, J.S., Menon, R.S., and Everling, S. (2011). Resting-state networks in the macaque at 7 T. Neuroimage *56*, 1546–1555.

Kagan, I., Iyer, A., Lindner, A., and Andersen, R.A. (2010). Space representation for eye movements is more contralateral in monkeys than in humans. Proc. Natl. Acad. Sci. USA *107*, 7933–7938.

Kamigaki, T., Fukushima, T., and Miyashita, Y. (2009). Cognitive set reconfiguration signaled by macaque posterior parietal neurons. Neuron *61*, 941–951.

Konishi, S., Wheeler, M.E., Donaldson, D.I., and Buckner, R.L. (2000). Neural correlates of episodic retrieval success. Neuroimage *12*, 276–286.

Koyama, M., Hasegawa, I., Osada, T., Adachi, Y., Nakahara, K., and Miyashita, Y. (2004). Functional magnetic resonance imaging of macaque monkeys performing visually guided saccade tasks: comparison of cortical eye fields with humans. Neuron *41*, 795–807.

Koyano, K.W., Machino, A., Takeda, M., Matsui, T., Fujimichi, R., Ohashi, Y., and Miyashita, Y. (2011). In vivo visualization of single-unit recording sites using MRI-detectable elgiloy deposit marking. J. Neurophysiol. *105*, 1380–1392.

Lewis, J.W., and Van Essen, D.C. (2000). Corticocortical connections of visual, sensorimotor, and multimodal processing areas in the parietal lobe of the macaque monkey. J. Comp. Neurol. *428*, 112–137.

Logothetis, N.K., Guggenberger, H., Peled, S., and Pauls, J. (1999). Functional imaging of the monkey brain. Nat. Neurosci. *2*, 555–562.

Maier, A., Wilke, M., Aura, C., Zhu, C., Ye, F.Q., and Leopold, D.A. (2008). Divergence of fMRI and neural signals in V1 during perceptual suppression in the awake monkey. Nat. Neurosci. *11*, 1193–1200.

Mantini, D., Gerits, A., Nelissen, K., Durand, J.B., Joly, O., Simone, L., Sawamura, H., Wardak, C., Orban, G.A., Buckner, R.L., and Vanduffel, W. (2011). Default mode of brain function in monkeys. J. Neurosci. *31*, 12954–12962.

Matsui, T., Koyano, K.W., Koyama, M., Nakahara, K., Takeda, M., Ohashi, Y., Naya, Y., and Miyashita, Y. (2007). MRI-based localization of electrophysiological recording sites within the cerebral cortex at single-voxel accuracy. Nat. Methods *4*, 161–168.

Matsui, T., Tamura, K., Koyano, K.W., Takeuchi, D., Adachi, Y., Osada, T., and Miyashita, Y. (2011). Direct comparison of spontaneous functional connectivity and effective connectivity measured by intracortical microstimulation: an fMRI study in macaque monkeys. Cereb. Cortex *21*, 2348–2356.

Matsui, T., Koyano, K.W., Tamura, K., Osada, T., Adachi, Y., Miyamoto, K., Chikazoe, J., Kamigaki, T., and Miyashita, Y. (2012). FMRI activity in the macaque cerebellum evoked by intracortical microstimulation of the primary somatosensory cortex: evidence for polysynaptic propagation. PLoS ONE *7*, e47515.

Miyashita, Y. (2004). Cognitive memory: cellular and network machineries and their top-down control. Science *306*, 435–440.

Nakahara, K., Hayashi, T., Konishi, S., and Miyashita, Y. (2002). Functional MRI of macaque monkeys performing a cognitive set-shifting task. Science *295*, 1532–1536.

Nelissen, K., Borra, E., Gerbella, M., Rozzi, S., Luppino, G., Vanduffel, W., Rizzolatti, G., and Orban, G.A. (2011). Action observation circuits in the macaque monkey cortex. J. Neurosci. *31*, 3743–3756.

Nelson, S.M., Cohen, A.L., Power, J.D., Wig, G.S., Miezin, F.M., Wheeler, M.E., Velanova, K., Donaldson, D.I., Phillips, J.S., Schlaggar, B.L., and Petersen, S.E. (2010). A parcellation scheme for human left lateral parietal cortex. Neuron *67*, 156–170.

Newman, M.E.J. (2006). Finding community structure in networks using the eigenvectors of matrices. Phys. Rev. E Stat. Nonlin. Soft Matter Phys. *74*, 036104.

Nichols, T., Brett, M., Andersson, J., Wager, T., and Poline, J.B. (2005). Valid conjunction inference with the minimum statistic. Neuroimage *25*, 653–660.

Nieder, A. (2005). Counting on neurons: the neurobiology of numerical competence. Nat. Rev. Neurosci. *6*, 177–190.

Osada, T., Adachi, Y., Kimura, H.M., and Miyashita, Y. (2008). Towards understanding of the cortical network underlying associative memory. Philos. Trans. R. Soc. Lond. B Biol. Sci. *363*, 2187–2199.

Paxinos, G., Huang, X.F., Petrides, M., and Toga, A.W. (2008). The Rhesus Monkey Brain in Stereotactic Coordinates (London: Elsevier Academic).

Peeters, R., Simone, L., Nelissen, K., Fabbri-Destro, M., Vanduffel, W., Rizzolatti, G., and Orban, G.A. (2009). The representation of tool use in humans and monkeys: common and uniquely human features. J. Neurosci. *29*, 11523–11539.

Petrides, M. (2005). Lateral prefrontal cortex: architectonic and functional organization. Philos. Trans. R. Soc. Lond. B Biol. Sci. *360*, 781–795.

Pinsk, M.A., DeSimone, K., Moore, T., Gross, C.G., and Kastner, S. (2005). Representations of faces and body parts in macaque temporal cortex: a functional MRI study. Proc. Natl. Acad. Sci. USA *102*, 6996–7001.

Rozzi, S., Calzavara, R., Belmalih, A., Borra, E., Gregoriou, G.G., Matelli, M., and Luppino, G. (2006). Cortical connections of the inferior parietal cortical convexity of the macaque monkey. Cereb. Cortex *16*, 1389–1417.

Rubinov, M., and Sporns, O. (2011). Weight-conserving characterization of complex functional brain networks. Neuroimage *56*, 2068–2079.

Rushworth, M.F.S., Behrens, T.E., and Johansen-Berg, H. (2006). Connection patterns distinguish 3 regions of human parietal cortex. Cereb. Cortex *16*, 1418–1430.

Smith, S.M., Fox, P.T., Miller, K.L., Glahn, D.C., Fox, P.M., Mackay, C.E., Filippini, N., Watkins, K.E., Toro, R., Laird, A.R., and Beckmann, C.F. (2009). Correspondence of the brain's functional architecture during activation and rest. Proc. Natl. Acad. Sci. USA *106*, 13040–13045.

Squire, L.R., Stark, C.E.L., and Clark, R.E. (2004). The medial temporal lobe. Annu. Rev. Neurosci. *27*, 279–306.

Stephan, K.E., Kamper, L., Bozkurt, A., Burns, G.A., Young, M.P., and Kötter, R. (2001). Advanced database methodology for the Collation of Connectivity data on the Macaque brain (CoCoMac). Philos. Trans. R. Soc. Lond. B Biol. Sci. *356*, 1159–1186.

Talmi, D., Grady, C.L., Goshen-Gottstein, Y., and Moscovitch, M. (2005). Neuroimaging the serial position curve. A test of single-store versus dual-store models. Psychol. Sci. *16*, 716–723.

Tsao, D.Y., Freiwald, W.A., Knutsen, T.A., Mandeville, J.B., and Tootell, R.B.H. (2003). Faces and objects in macaque cerebral cortex. Nat. Neurosci. *6*, 989–995.

Vanduffel, W., Fize, D., Peuskens, H., Denys, K., Sunaert, S., Todd, J.T., and Orban, G.A. (2002). Extracting 3D from motion: differences in human and monkey intraparietal cortex. Science *298*, 413–415.

Vilberg, K.L., and Rugg, M.D. (2008). Memory retrieval and the parietal cortex: a review of evidence from a dual-process perspective. Neuropsychologia *46*, 1787–1799.

Vincent, J.L., Snyder, A.Z., Fox, M.D., Shannon, B.J., Andrews, J.R., Raichle, M.E., and Buckner, R.L. (2006). Coherent spontaneous activity identifies a hippocampal-parietal memory network. J. Neurophysiol. *96*, 3517–3531.

Vincent, J.L., Patel, G.H., Fox, M.D., Snyder, A.Z., Baker, J.T., Van Essen, D.C., Zempel, J.M., Snyder, L.H., Corbetta, M., and Raichle, M.E. (2007). Intrinsic functional architecture in the anaesthetized monkey brain. Nature *447*, 83–86.

Wagner, A.D., Desmond, J.E., Glover, G.H., and Gabrieli, J.D. (1998). Prefrontal cortex and recognition memory. Functional-MRI evidence for context-dependent retrieval processes. Brain *121*, 1985–2002.

Wagner, A.D., Shannon, B.J., Kahn, I., and Buckner, R.L. (2005). Parietal lobe contributions to episodic memory retrieval. Trends Cogn. Sci. *9*, 445–453.

Wright, A.A., Santiago, H.C., Sands, S.F., Kendrick, D.F., and Cook, R.G. (1985). Memory processing of serial lists by pigeons, monkeys, and people. Science *229*, 287–289.

Yonelinas, A.P., Otten, L.J., Shaw, K.N., and Rugg, M.D. (2005). Separating the brain regions involved in recollection and familiarity in recognition memory. J. Neurosci. *25*, 3002–3008.